THE JOURNAL OF PHYSICAL CHEMISTRY C LETTERS

2008, *112,* 11082–11085
Published on Web 07/08/2008

Solution-Processed Zinc Tin Oxide Semiconductor for Thin-Film Transistors

Sunho Jeong, Youngmin Jeong, and Jooho Moon*

Department of Materials Science and Engineering, Yonsei University, 134 Shinchon-dong Seodaemun-gu, Seoul 120-749, Korea

Received: April 22, 2008; Revised Manuscript Received: June 14, 2008

A zinc tin oxide (ZTO) semiconductor layer for thin-film transistor was fabricated using solution-processable sol−gel material. To obtain semiconductor characteristics, ZTO gels should be annealed such that salts and organic components in the ZTO layer undergo complete decomposition. The thermal behavior of ZTO precursor materials was investigated, and the electrical performances of solution-processed transistors were analyzed as a function of the annealing temperature of the ZTO semiconductor layer. We also studied the electrical performance of transistors as a function of the Sn content of the ZTO layer, in order to understand its influence on the device characteristics of solution-processed transistors.

Introduction

Interest in novel thin-film transistors for developing low-cost, lightweight, and printable electronics, such as paper-like display, radio frequency identification tags, and large-area sensors, has significantly increased.[1,2] However, hydrogenated amorphous silicon (a-Si:H), which has been commonly used as a semiconductor layer for conventional thin-film transistors,[3,4] has several limitations including low mobility, high photosensitivity, and high-cost due to its vacuum deposition process.[5] High manufacturing costs in particular pose an obstacle for the realization of modern large-area and mass-produced electronics. In contrast, solution-processed deposition of semiconductor layers offers many advantages such as simplicity, low-cost, and high throughput, thus enabling the fabrication of flexible low-cost electronics. Various solution-processed organic semiconductor materials have therefore been extensively researched. However, organic semiconductors are generally sensitive to operating circumstances and unstable during long-term operation.[6–10]

Recently, ZnO-based materials have been researched as solution-processed and high-performance semiconductor materials. The conduction band of ZnO-related materials is primarily composed of spatially spread large metal 4s orbitals with isotropic shape, and therefore, carriers can be directly transported through overlapped neighboring metal orbitals, whereas the carrier transport in a-Si:H is controlled by hopping between localized tail-states, and band conduction is prohibited.[11–13] Most research has focused mainly on ZnO[14–16] and zinc indium oxide (IZO)-based thin film transistors,[17] which exhibit a mobility of $\sim 5\ cm^2\ V^{-1}\ s^{-1}$. However, little work has been conducted on ZTO except for the recent study by Chang et al.[18] They synthesized solution-processed ZTO materials using chlorides as starting precursors. Although their ZTO-based transistors demonstrated reasonable electrical performance, chloride compounds can leave very toxic byproduct behind. In this article, we report solution-processed ZTO-based thin film transistors derived from acetate salts. The structural evolution of the ZTO sol−gel precursor was monitored as a function of annealing temperature under ambient atmosphere, and its influence on the electrical performance of transistors was investigated. In addition, we studied the variation of transistor performance as a function of Sn doping concentration.

Experimental Section

Precursor solutions for the ZTO semiconductor layer were synthesized from zinc acetate dehydrate ($Zn(CH_3COO)_2 \cdot 2H_2O$) and tin acetate ($Sn(CH_3COO)_2$) dissolved in 2-methoxyethanol. The concentration of metal precursors was 0.75 M, and the molar ratio of (Sn/Sn+Zn) was varied from 0.2 to 0.4. Ethanolamine was used as stabilizing agents to improve the solubility of precursor salts. The solution was stirred for 12 h at room temperature and then filtered through a 0.2-μm membrane (PTFE, Advantec MFS) prior to spin-coating. The precursor solution was spin-coated on heavily doped silicon substrates with 200-nm-thick SiO_2 as a dielectric layer/gate electrode. The films obtained had a thickness of ~35 nm, and were dried at 95 °C for 90 s to evaporate solvent. They were then annealed at temperatures ranging from 300 to 600 °C in air. To fabricate top-contact thin-film transistors, Al source/drain electrodes were vacuum-deposited via a shadow mask on top of the ZTO layer on SiO_2/n^+-Si. The width and length of the channel were 3 mm and 100 μm, respectively. A postannealing step at 200 °C under an $H_2 + N_2$ atmosphere was performed to improve the electrical performance of the transistor prior to the measurement. $I-V$ characteristics, and the electrical performance of transistors were determined using an Agilent 5263A source-measure unit.

The thermal decomposition behavior of the sol−gel precursors was monitored using thermal gravimetric analysis (TGA) and differential scanning calorimetry (DSC, STA409C, Netzsch). Thermal analysis was conducted under ambient atmosphere. Phase transformation and crystallization were measured using high resolution X-ray diffraction (X'Pert-PRO MRD, Phillips) and HR-TEM (JEM-4010, JEOL). The grain size and surface morphology were observed by both atomic force microscopy

* Corresponding author. Tel.: +82-2-2123-2855. Fax: +82-2-365-5882. E-mail: jmoon@yonsei.ac.kr.

10.1021/jp803475g CCC: $40.75

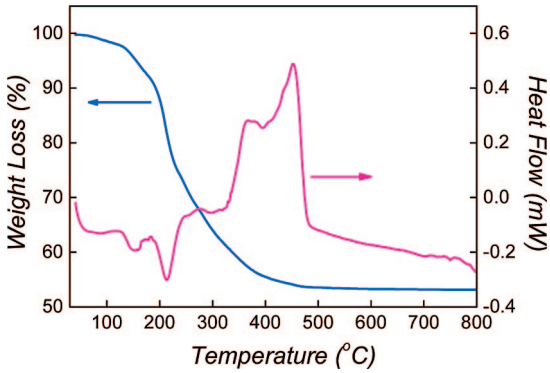

Figure 1. TGA and DSC curves of ZTO precursor material. The Sn concentration in the ZTO precursor is 30 mol %.

(AFM, SPA 400, Seiko) and scanning electron microscopy (JSM-6500F, JEOL).

Results and Discussion

Figure 1 shows the thermal behavior of ZTO precursor material doped with 30 mol % Sn, determined by TG/DSC analyses. The weight loss that occurred below 200 °C can be attributed to the evaporation of both solvent and organic additive incorporated into the ZTO precursor, because the boiling points of solvent and organic additive are either below or around 200 °C. The abrupt weight loss observed above 200 °C represents the thermal decomposition of both the complex ligands originating from the stabilizing agent and the organic group associated with the metal acetates. Decomposition was completed at around 500 °C. Thermal behavior analysis of the ZTO precursor material revealed that semiconductor characteristics were present only after annealing at temperatures above 500 °C, because, below this temperature, both solvent and organic molecule residues can act as obstacles for charge carrier accumulation and transportation in the conduction band.

ZTO precursor material can also undergo phase transformation from amorphous to crystalline states during annealing. Taking into consideration the fact that there were no exothermic or endothermic peaks in thermal analysis, indicative of the absence of phase transformation, we believe that the ZTO layer remains in an amorphous phase without forming any secondary phase regardless of annealing temperature. However, this assumption could be incorrect since the determination of phase transformation based on thermal behavior is indirect, and the DSC peak which is attributed to phase transition can be overlapped by other peaks due to thermal decomposition of organic components. Therefore, to verify whether phase transformation occurs during annealing, we analyzed high-resolution X-ray diffraction patterns of ZTO thin films annealed at temperatures ranging from 300 to 500 °C, shown in Figure 2. The X-ray diffraction profiles exhibited three amorphous-like broad peaks located at around 20°, 33°, and 56°, and sharp crystalline peaks were observed at 51.5° and 54.5°. Their peak positions and intensities remained relatively unchanged regardless of the annealing temperature. Strong crystalline peaks at 51.5° and 54.5° originated from the substrate of SiO_2(thickness = 200 nm)/Si(100). The amorphous-like broad peaks encompassed the major diffraction peaks for crystalline $ZnSnO_3$, Zn_2SnO_4, and SnO_2, consistent with the previous report by Chiang et al.,[19] in which they claimed that the ZTO had an amorphous structure rather than a crystalline structure.

It has been reported that the incorporation of additional elements (such as In, Sn, Ga, or Al) in a crystalline ZnO matrix induces the transformation of crystalline phase into an amorphous phase.[20,21] Excessive doping can lead to the formation of secondary phases (the solubility limit depends on the material composition and is generally 5−10 at. %). However, the presence of secondary phases does not deteriorate the characteristic of carrier transportation, since the conduction band minimum in amorphous ZnO is composed of vacant s orbital of cation.[11,12,22] In our material system, the incorporated Sn at the content of 10−40 mol% also transforms the ZnO matrix into the amorphous phase, together with the formation of secondary phases (possibly trigonal ilmenite $ZnSnO_3$ and/or cubic spinel Zn_2SnO_4). The thermally unstable $ZnSnO_3$ phase might partially decompose into Zn_2SnO_4 and SnO_2.[19,23] However, the presence of amorphous-like broad peaks indicates that the secondary phases are also amorphous or very small crystallites. Therefore, it is reasonable to state that the ZTO is composed of an amorphous phase at temperatures between 300 and 500 °C. HR-TEM observation was in good agreement with the XRD result as shown in Figure 2b. The ZTO film annealed at 500 °C was composed of amorphous materials in which approximately 1∼2 nm sized particles were embedded. Selective area diffraction revealed only amorphous ring structure (Figure 2c).

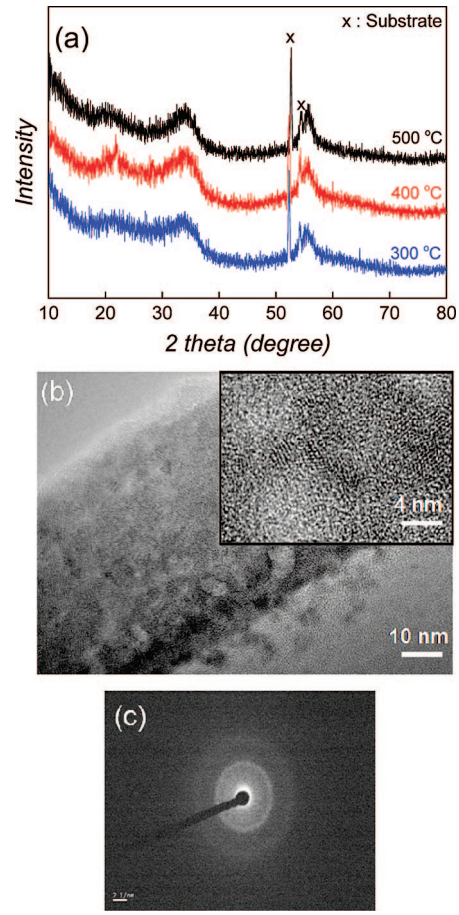

Figure 2. (a) High resolution X-ray diffraction patterns obtained from ZTO layers annealed at 300, 400, and 500 °C. The Sn concentration of the ZTO films is 30 mol%, and the incident angle is 1°. (b) HR-TEM image and (c) selective area diffraction pattern of ZTO layer annealed at 500 °C. The inset in Figure 2b is a magnified HR-TEM image.

Figure 3a shows the electrical performances of transistors incorporating the sol−gel-derived ZTO layers (Sn 30 mol%) annealed at various temperatures between 300 and 500 °C. Since degenerate band conduction is possible in amorphous oxide

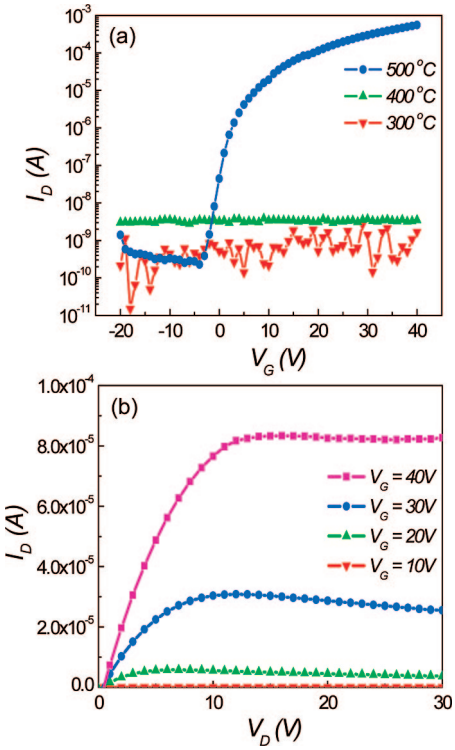

Figure 3. (a) Transfer characteristics of transistors fabricated using the ZTO layer annealed at different temperatures ranging from 300 to 500 °C and (b) output characteristic of transistor fabricated using a ZTO layer annealed at 500 °C. The Sn concentration of the ZTO films is 30 mol %.

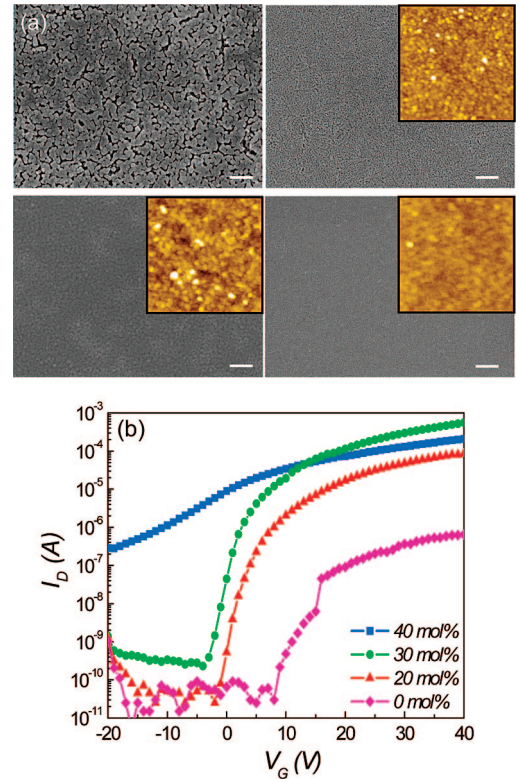

Figure 4. (a) SEM images of sol−gel derived ZTO films as a function of the Sn content. The insets are the corresponding AFM images. The images in clockwise direction correspond to 0, 20, 30, and 40 mol%, respectively. The scale bar presents 200 nm in SEM image, whereas 95 nm in AFM image. (b) Transfer characteristics of transistors fabricated using ZTO layers with different Sn concentrations ranging from 0 to 40 mol%. All ZTO layers were annealed at 500 °C.

TABLE 1: Electrical Performance Parameters of Transistors Fabricated Using a ZTO Layer with Sn Concentrations Ranging from 0 to 30 mol%[a]

Sn concentration	μ_{FET} ($cm^2\ V^{-1}\ s^{-1}$)	V_T (V)	I_{on} (A)	$I_{on/off}$
0 mol%	0.002	9.05	6×10^{-7}	10^4
20mol%	0.3	6.0	8×10^{-5}	10^6
30mol%	1.1	1.9	5×10^{-4}	10^6

[a] All ZTO layers were annealed at 500 °C.

semiconductors containing post-transition-metal cations,[11,12] we predicted that the ZTO layer could behave as a semiconductor material if the organic substances incorporated into it underwent complete thermal decomposition. As predicted, the ZTO layers annealed at 300 and 400 °C behaved as an insulators rather than semiconductors, whereas the transistor based on ZTO annealed at 500 °C showed the typical electrical characteristics of an n-channel transistor. As shown in Figure 3b, the solution-processed ZTO transistor at 500 °C was well-modulated depending on the gate voltage and exhibited clear linear/saturation behavior with a field-effect mobility of 1.1 $cm^2\ V^{-1}\ s^{-1}$, on/off ratio of 10^6, off-current of 3×10^{-10} A, and threshold voltage of 1.9 V.

The electrical performance of transistors with ZTO as a semiconductor layer can also be influenced by the carrier concentration. The amount of charge carriers is controlled by oxygen-vacancy formation via annealing under a reducing atmosphere; in particular, hydrogen can act as both a shallow donor and a defect passivator in ZnO-based material. However, charge carriers generated by reduction are sensitive to process conditions, which make it difficult to precisely control their concentrations. However, charge carriers could increase as a function of the Sn concentration, because Sn has two more valence electrons than Zn, and Sn acts as a donor by either substituting for the Zn atom or occupying the interstitial sites.

To analyze the electrical performance of transistors as a function of Sn concentration, we fabricated the transistor using ZTO with different Sn contents ranging from 0 to 40 mol %. The microstructure of the sol−gel-derived ZTO films with varying Sn content is shown in Figure 4a. Undoped ZnO film (0 mol% Sn) had a porous structure in which the grain size was approximately 50 nm and a rms roughness determined by $500 \times 500\ nm^2$ area AFM scan is 67 nm. Addition of Sn significantly improved the surface smoothness by decreasing the grain size. The rms value for the 20 mol% ZTO was 12.1 nm, whereas 10.3 and 6.4 nm for the 30 mol% ZTO and 40 mol% ZTO, respectively. There are no noticeable differences in the grain sizes (approximately 5 nm) for the ZTO films doped with 20, 30, and 40 mol% Sn.

The transfer characteristics of transistors involving the sol−gel-derived ZTO are depicted in Figure 4b, and the calculated electrical parameters such as field-effect mobility, threshold voltage, on-current, and on/off ratio are shown in Table 1. Field-effect mobility increased with increasing Sn concentration (from 0 to 30 mol%), which was presumably because of more charge carrier generation by either substitution of Zn^{2+} lattice sites by ions, or the occupation of interstitial sites by Sn^{4+} ions. The extremely low mobility associated with undoped ZnO film can be attributed to grain boundary scattering due to less-dense microstructure. On the other hand, it was observed that the threshold voltage shifts toward negative gate bias with increasing Sn concentration. Since the threshold voltage is defined as the voltage required to accumulate sufficient charge carriers to form a conductive channel path, the presence of more

charge carriers enables channel formation at a lower gate bias, resulting in the threshold voltage shift. The charge carrier generation was also responsible for the fact that the 30 mol% Sn-doped ZnO based transistor displayed higher off-current than the 20 mol% Sn-doped ZnO based transistor. Higher charge carrier concentration decreased the resistivity of the ZTO layer, which in turn resulted in a higher off-current under the depletion mode (i.e., negative gate bias). However, as the Sn content reached 40 mol%, the transistor exhibited abnormal behavior. Doping with excess Sn made the ZTO layer to be conductive rather than semiconductive. Even under a high negative bias, the depletion of the channel region was incompletely fulfilled, as indicated by even higher off-current.

Conclusions

We synthesized a sol−gel-derived precursor solution to create a ZTO semiconductor material using acetate salts and appropriate organic additive. We confirmed that the thermal decomposition of organic residues was complete via annealing up to 500 °C and demonstrated that the resulting ZTO films are composed mainly of an amorphous phase, regardless of the annealing temperatures. We further demonstrated that the transistor fabricated using the spin-cast ZTO layer annealed at 500 °C exhibits typical semiconductor behavior with a field-effect mobility of 1.1 $cm^2\ V^{-1}\ s^{-1}$, an on/off ratio of 10^6, an off-current of 3×10^{-10} A, and a threshold voltage of 1.9 V. In addition, we found that the electrical characteristic of the ZTO transistor was influenced by the Sn concentration. The addition of 30 mol% Sn was optimal for obtaining better transistor performance.

Acknowledgment. This work was supported by a grant from the Korean Science and Engineering Foundation (KOSEF) through the National Research Laboratory Program funded by the Ministry of Education, Science Technology (No. R0A-2005-000-10011-0). This research was also partially supported by LG Display and the Second Stage of the Brain Korea 21 Project.

References and Notes

(1) Huitema, H. E. A.; Gelinck, G. H.; Van Der Putten, J. B. P. H.; Kuijk, K. E.; Hart, C. M.; Cantatore, E.; Herwig, P. T.; Van Breemen, A. J. J. M.; de Leeuw, D. M. *Nature* **2001**, *414*, 599.
(2) Chen, Y.; Au, J.; Kazlas, P.; Ritenour, A.; Gates, H.; McCreary, M. *Nature* **2003**, *423*, 136.
(3) McCormick, C. S.; Weber, C. E.; Abelson, J. R.; Gates, S. M. *Appl. Phys. Lett.* **1997**, *70*, 226.
(4) Gleskova, H.; Wagner, S.; Gasparik, V.; Kovac, P. *J. Electorchem. Soc.* **2001**, *148*, G370.
(5) Kakinura, H. *Phys. Rev. B* **1989**, *39*, 10473.
(6) Gu, G.; Kane, M. G.; Doty, J. E.; Firester, A. H. *Appl. Phys. Lett.* **2005**, *87*, 243512.
(7) Zilker, S. J.; Detcheverry, C.; Cantatore, E.; de Leeuw, D. M. *Appl. Phys. Lett.* **2001**, *79*, 1124.
(8) Backlund, T. G.; Osterbacka, R.; Stubb, H.; Bobacka, J.; Ivaska, A. *J. Appl. Phys.* **2005**, *98*, 074504.
(9) Sekitani, T.; Iba, S.; Kato, Y.; Noguchi, Y.; Someya, T.; Sakurai, T. *Appl. Phys. Lett.* **2005**, *87*, 073505.
(10) Salleo, A.; Endicott, F.; Street, R. A. *Appl. Phys. Lett.* **2005**, *86*, 263505.
(11) Nomura, K.; Ohta, H.; Takagi, A.; Kamiya, T.; Hirano, M.; Hosono, H. *Nature* **2004**, *432*, 488.
(12) Nomura, K.; Takagi, A.; Kamiya, T.; Ohta, H.; Hirano, M.; Hosono, H. *Jpn. J. Appl. Phys* **2006**, *45*, 4303.
(13) Martins, R.; Barquinha, P.; Ferreira, I.; Pereira, L.; Goncalves, G.; Fortunato, E. *J. Appl. Phys.* **2007**, *101*, 044505.
(14) Ong, B. S.; Li, C.; Li, Y.; Wu, Y.; Loutfy, R. *J. Am. Chem. Soc.* **2007**, *129*, 2750.
(15) Cheng, H.-C.; Chen, C.-F.; Tsay, C.-Y. *Appl. Phys. Lett.* **2007**, *90*, 012113.
(16) Lee, D.-H.; Chang, Y.-J.; Herman, G. S.; Chang, C.-H. *Adv. Mater.* **2007**, *19*, 843.
(17) Choi, C. G.; Seo, S.-J.; Bae, B.-S. *Electrochem. Solid State Lett.* **2008**, *11*, H7.
(18) Chang, Y.-J.; Lee, D.-H.; Herman, G. S.; Chang, C.-H. *Electrochem. Solid State Lett.* **2007**, *10*, H135.
(19) Chiang, H. Q.; Wager, J. F.; Hoffman, R. L.; Jeong, J.; Keszler, D. A. *Appl. Phys. Lett.* **2005**, *86*, 013503.
(20) Kim, D. H.; Cho, N. G.; Kim, H. G.; Choi, W.-Y. *J. Electrochem. Soc.* **2007**, *154*, H939.
(21) López-Ponce, E.; Costa-Krämer, J. L.; Martin-González, M. S.; Briones, F.; Fernandez, J. F.; Caballero, A. C.; Villegas, M.; de Frutos, J. *Phys. Stat. Sol. (a)* **2006**, *203*, 1383.
(22) Nomura, K.; Jamiya, T.; Ohta, H.; Uruga, T.; Hirano, M.; Hosono, H. *Phys. Rev. B* **2007**, *75*, 035212.
(23) Minami, T.; Takata, H.; Sato, H.; Sonohara, H. *J. Vac. Sci. Technol. A* **1995**, *13*, 1095.

JP803475G